PNC-TN9410 88-014

Experimental Study on Penetration Behaviors of Water Jet into Freon-11 and Liquid Nitrogen〔I〕

——Summary——

Junuary, 1988

OARAI ENGINEERING CENTER

POWER REACTOR AND NUCLEAR FUEL DEVELOPMENT CORPORATION

複製又はこの資料の入手については，下記にお問い合わせください。
〒311-13　茨城県東茨城郡大洗町成田町4002
動力炉・核燃料開発事業団
大洗工学センター　システム開発推進部・技術管理室

Enquires about copyright and reproduction should be addressed to: Technology Management Section O-arai Engineering Center, Power Reactor and Nuclear Fuel Development Corporation 4002 Narita-cho, O-arai-machi, Higashi-Ibaraki, Ibaraki-ken, 311-13, Japan

動力炉・核燃料開発事業団（Power Reactor and Nuclear Fuel Development Corporation）

PNC-TN9410 88-014
1988 年 1 月

Experimental Study on Penetration Behaviors of Water Jet into Freon-11 and Liquid Nitrogen〔I〕

——Summary——

斉藤 正樹*，佐藤 浩司*
今堀 真司*

要 旨

溶融炉心物質が，下部の冷却材中にジェット状に落下する際の冷却材中への浸入挙動を調べるため，約 90 ℃の高温水ジェットをフレオン－11 中に，また，室温の水ジェットを液体窒素中に注入する基礎試験を実施し，その浸入挙動を高速度ビデオ（200 コマ／秒）で観測した。

本試験の結果より以下のことが明らかになった。

(1) 冷却材中への高温ジェットの浸入距離は，ジェットの流速，ジェットの径および冷却材の密度に対するジェットの密度比が増すに従って増加する。

(2) ジェット径で無次元化した浸入距離は，フルード数，ジェットと冷却材の密度比によって以下のような相関式として表わされる。

$$L/D_j = 2.1\,(\rho_j/\rho_c)^{0.5}\,F_r^{0.5}$$

(3) 高温溶融ジェットの冷却材中への浸入挙動において，発生する蒸気が非常に重要な役割をする。すなわち，Rayleigh－Taylor 型不安定性によってジェット先端で発生する蒸気がジェットの側部を囲み，ジェットと冷却材との接触を防げる結果，ジェットの冷却材中への浸入を助ける。一方，ジェットの側部において，蒸気を介して冷却材との相互作用によって生ずる Kelvin－Helmholtz 型不安定性は，ジェットの冷却材中への浸入を防げる働きをする。

* 動力炉・核燃料開発事業団，大洗工学センター，安全工学部，高速炉安全工学室

PNC-TN9410 88-014
JANUARY 1988

Experimental Study on Penetration Behaviors of Water Jet into Freon-11 and Liquid Nitrogen [I]

— Summary —

Masaki Saito*, Koji Sato*
Shinji Imahori*

ABSTRACT

To investigate the fundamental physical phenomena on the penetration behaviors of a large molten core jet into coolant, the experiments have been performed by using water jets into freon-11 and liquid nitrogen. A hot water jet of 90 °C was injected into freon-11 at room temperature with various velocities from 2.5 m/s to 15 m/s through a nozzle with various diameters from 5 mm to 40 mm. To examine the effects of density difference between the jet and the coolant on the jet penetration behaviors, additional experiments were performed with a water jet at room temperature and liquid nitrogen pool.

From the present experiments, it is found that the penetration length of the jet into coolant tends to increase with the jet velocity, the jet diameter and the density ratio between the jet and coolant. The relative penetration length normalized by the jet diameter can be correlated well with the Froude number and the density ratio between the jet and the coolant:

$$L/D_j = 2.1(\rho_j/\rho_c)^{0.5}\ Fr^{0.5}$$

This correlation can also predict well the experimental results of the breakup length which were obtained by Spencer et al. with very heavy jets such as Wood's metal injected into water pool.

---

* FBR Safety Engineering Section, Safety Engineering Division, O-arai Engineering Center, Power Reactor and Nuclear Fuel Development Corporation

It is also concluded that the behaviors of the vapor play an important role in the penetration process of the hot jet into coolant. In the case of mild FCIs such as present experiments, blanketing of the jet by the vapor generated at the leading edge due to the Rayleigh-Taylor type instability tends to prevent the jet from contacting with the coolant at the vertical trailing column of the jet, which helps the jet to penetrate into the coolant. On the other hand, the Kelvin-Helmholtz type instability increases the hydrodynamic interactions between the vertical trailing jet column with the coolant, resulting in small penetration of the jet into the coolant.

I. INTRODUCTION

It is very important to provide the technical data base and more reliable theoretical tools in order to assess the inherent retentionability of the molten core materials without leading to vessel failure and release of the large amount of radioactive materials after permanent shutdown in LMFBR severe accidents. A very desirable goal of this kind of researches is to confirm and moreover to ascertain the plant safety margins by sophisticated design without additional engineered safety features for this kind of very unlikely severe accidents in LMFBR.

After a permanent shutdown is achieved by the fuel dispersal from the active core region, the remaining molten core materials may either be encapsuled by the crust in the core assembly region to be cooled down by the ambient coolant and the cold core structures, or penetrate the core assembly in downward direction by the effects of the gravity and residual decay heat generation and discharge into the lower plenum.

In this meaning, the following phenomena are important in the PAMR (Post-Accident Materials Relocation) phase:

(1) molten core-pool behaviors such as
   - pool separation due to the density difference between fuel and structural materials (stainless steel)
   - melting front propagation of the molten pool, and

(2) thermal and hydrodynamic interactions between molten core materials and coolant/structures during the relocation process of the hot debris in the lower plenum.

In the second part of the key phenomena, a great concern is the potential direct contact of a molten fuel jet, which is released from the bottom of the core through the control rod assemblies which have weaker thermal resistance in the lower axial blanket region in LMFBR, with structures located underneath the core assembly.

Therefore, a particular emphasis should be placed on the investigation of the breakup or penetration behaviors of a large molten core material jet in the coolant, and also on the erosion behaviors of the structures by a large molten core material jet.

The hydrodynamic instability contributes to the jet breakup. Many theoretical and experimental studies have been performed by Rayleigh[1], Weber[2], Fenn et al.[3], Grant et al.[4], Phinney[5] and Meister et al.[6], which are summarized by McCarthy and Molloy[7].

Most of these studies were performed under isothermal condition between the jet with relatively small diameter and the continuum field. Under the anisothermal condition such as the interaction between molten core material jets and coolant, the behaviors of the vapor generated may play an important role in the penetration and breakup processes of the hot jet in the coolant. The jet may be fragmented by the vapor explosion before reaching the long penetration. On the other hand, in the mild vapor generation, the vapor may prevent the hot jet from contacting with coolant to help the penetration into coolant. In some conditions, the jet may be cooled to form the crust on the surface before the fragmentation.

Therefore, in the penetration process of the molten core material jet into the coolant, the following effects are of great concern:

(1) Hydrodynamic instability and the breakup (or entrainment) not only at the vertical trailing column but also at the leading edge, especially in the case of the jet with large diameter,
(2) Anisothermal interactions (stable film boiling ?, vapor blanketing ?, energetic FCI ?),
(3) Density difference between the jet and the coolant,
(4) Crust formation on the jet surface,
(5) Scaling effects (ratio of the jet diameter to the coolant depth).

The concept of the leading edge breakup and several kinds of hydrodynamic instabilities were first proposed by Theofanous and Saito[8] in conection with the molten jet penetration behaviors into coolant. Some other experimental and theoretical researches have been performed by Marten et al.[9], Spencer et al.[10], Bradley[11] and Epstein et al.[12] The penetration and breakup behaviors of a hot and large jet in the coolant, however, have not been well understood.

Therefore, a series of the model experiments on the interaction between the molten jet and coolant/structure is in progress at PNC at low (<500 °C) and high (1000 °C ∿ 2300 °C) temperatures.

The present paper deals with the results of the preliminary model experiments at low temperature which were performed by using water as a jet, and freon-11 and liquid nitrogen as coolant, to understand the fundamental physical phenomena of the penetration behaviors of a large molten jet into coolant.

II. EXPERIMENTS

The experiments were conducted in the facility (JET-I) shown in Fig. 1, which consists of the heating tank, the nozzle section, the test section and the N_2 gas line. The heating tank can be heated up to 300 °C by the Nichrome heaters and pressurized up to 10 kg/cm^2 to control the jet velocity. About 200 liters of jet materials such as water and molten Wood's metal can be injected into the coolant simulant through a long nozzle with Nichrome heaters and thermal insulations, which is detachable to change the jet diameter up to 100 mm.

The inner vessel at the test section with 120 cm height and 30 cm × 30 cm cross section is surrounded by the thermal insulations for the liquid nitrogen tests. Two side walls were made of special lucite plastic plates for observing jet penetration behaviors into the coolant by a high-speed video camera with 200 frames per second.

The initial coolant level was always set to the lower edge of the nozzle to avoid the entrapments of air. One of the blind walls was cut for overflowing and keeping the coolant surface level constant during the experiments.

The outer vessel with 170 cm height and 51 cm × 51 cm cross section was installed for the coolant overflow and for the protection of the measuring systems.

A hot water jet of about 90 °C was injected into freon-11 at room temperature with various velocities from 2.5 m/s to 15 m/s through a nozzle with various diameters from 5 mm to 40 mm. To investigate the influence of the density difference between the jet and the coolant, additional experiments were performed with a water jet at room temperature and liquid nitrogen pool.

The experimental conditions are shown in Tables 1 and 2.

III. EXPERIMENTAL RESULTS AND DISCUSSIONS

1. Overview of the penetration behaviors

The typical initial penetration behaviors of a hot water jet into freon-11 are shown in Fig. 2. The time interval between the pictures is 20 msec. The picture at the left end on the top line shows the behavior

of a jet with the same experimental conditions falling in the air. When the hot jet penetrates into coolant, most of the vapor is produced at the leading edge, which immediately surrounds the vertical trailing column of the jet. It is clearly seen, however, in these figures that although the instability induced at the boundary between the vapor and the ambient coolant tends to breakup the jet, the jet penetration develops again, and that the thick jet blanketing by the vapor helps the penetration of the jet into the coolant because the vapor layer prevents the jet stream from interacting directly with the ambient coolant.

The good reproducibility of the experiments is shown in Fig. 3. After initial jet penetration is developed, the position of the leading edge stays with small fluctuations, where the forces are balanced among the jet initial inertia, the buoyancy due to the density difference between the jet and coolant, and the other force due to the hydrodynamic interactions between the jet and the vapor flows, which will be discussed later more thoroughly.

Figures 4 and 5 show the influence of jet velocity on the penetration behaviors into freon-11 and liquid nitrogen pools, respectively. The velocity of the leading edge in the initial penetration, the final penetration depth and the fluctuation level of the leading edge tend to increase with the original jet velocity. No or very slight overshoot of the initial penetration was seen in the cases of the lower jet velocity. It tends to appear, however, with the jet injection velocity and the degree of the subcooling of freon-11 as seen in Fig. 3. The almost similar tendencies are seen for the influences of the jet velocity in liquid nitrogen pool. The jet with the same injection velocity, however, penetrates more deeply in the liquid nitrogen than in the freon-11 pool, because of the density difference between the jet and the coolant, which will be discussed more in detail in later section.

The effects of the jet diameter on the penetration behaviors were shown in Fig. 6. With inceasing the size of the jet, the penetration depth and the oscillation level of the leading edge tends to increase. The velocity of the leading edge during the initial penetation, however, tends to be independent of the jet diameter.

In most cases except for a few data with 5 mm$^{\phi}$ jet size, the velocity of the leading edge in the initial penetration stage reduced to almost half of the original jet velocity. This means that almost half of the jet mass flow from the nozzle may be entrained into the vapor and carried

away by the vapor flow from the jet stream or that the diameter of the jet must be roughly 1.5 times of the original one during the initial penetration.

From these observations, as pointed out previously by Theofanous and Saito[8], and Theofanous et al.[13], it will be concluded that some of the jet material may be stripped from the jet stream and mixed with the vapor flow during the penetration into coolant, however, that the undisturbed jet body is still continuous within the vapor blanket except the highly broken-up leading edge.

2. Penetration length

The penetration length (L) of the jet into coolant was estimated as a mean value of the depth of the leading edge because slight oscillations were observed after established complete steady-state jet. In Fig. 7, the penetration lengths with the standard deviation are shown as a function of the original jet velocity with jet diameter as a parameter. From these figures, it is clearly seen that the penetration length tends to increase linearly with the jet velocity. It is also seen that the penetration length tends to increase with the jet diameter. In Fig. 7(a), the penetration lengths in the cases of the water jet into the liquid nitrogen pool are compared with those in the cases of the water jet into the freon-11 pool. The penetration lengths in the liquid nitrogen are longer than those in the freon-11.

All the results are summarized in Fig. 8, where the normalized penetration lengths by the jet diameter and the square root of the density ratio of the jet to the coolant are plotted as a function of the Froude number defined by $Fr = U_j^2/g\ D_j$. From this figure, it is concluded that the relative penetration length normalized by the jet diameter can be correlated well with the Froude number and the density ratio between the jet and the coolant:

$$L/D_j = 2.1(\rho_j/\rho_c)^{0.5}\ Fr^{0.5}\ . \qquad (1)$$

In Fig. 8, two experimental results of the breakup length in the case of the heavy metal jets injected into water are also plotted, which were observed by the Hycamn camera in the experiments conducted by Spencer et al.[10] with Wood's metal (50% bismuth, 25% lead, 12.5% tin

and 12.5% cadmium; ρ_j = 9200 kg/m^3) and Cerrotru (a eutectic, 58% bismuth and 42% tin; ρ_j = 8670 kg/m^3) jets. Figure 8 shows that the correlation of Eq. (1) can also predict well the breakup lengths of the jet in the case of higher density ratio of the jet to the coolant.

3. Thermal and hydrodynamic interactions between jet and coolant

When a jet penetrates into coolant, it always receives the resistant forces such as buoyancy due to the density difference $((\rho_c-\rho_j)g)$ and other force, $(\Delta P/\Delta \ell)_f$, due to thermal and hydrodynamic interactions between the jet and coolant. As shown in Fig. 9, if these resistant forces can balance steadily with the jet initial inertia at the depth in the coolant, where the velocity of the jet leading edge is zero, the penetration length (L) can be expressed:

$$\frac{1}{2}\rho_j V_j^2 = (\rho_c-\rho_j)gL + \left(\frac{\Delta P}{\Delta l}\right)_f L \ , \tag{2}$$

$$L/D_j = \frac{1}{2}\cdot\frac{\rho_j}{(\rho_c-\rho_j)}\cdot Fr\cdot K_p \ , \tag{3}$$

where $Fr = V_j^2/gD_j$: Froude number,

$K_p = 1/(1-K_i)$: Penetration Parameter, (4)

and $K_i = \left(\frac{\Delta P}{\Delta l}\right)_f/(\rho_j-\rho_c)g$: Interaction Parameter. (5)

K_i defined by Eq. (5), which is named as Interaction Parameter, indicates the relative strength of the resistant force due to the thermal and hydrodynamic interactions between the jet and the coolant, compared with the buoyancy due to the density difference. On the other hand, K_p defined by Eq. (4), which is also named as Penetration Parameter, indicates the degree of the jet penetration into the coolant. The relationship between Interaction Parameter and Penetration Parameter is shown in Fig. 10.

In the case of the injection of a jet with lower density than that of the coolant, as the resistant force due to the thermal and hydrodynamic interactions between the jet and the coolant becomes weaker and weaker, that is $(\Delta P/\Delta l)_f \to 0$, Interaction Parameter K_i approaches to zero and Penetration Parameter K_p approaches to 1. When the resistant force due

to the thermal and hydrodynamic interactions between the jet and the coolant is very small and ignored compared with buoyancy, the penetration length is determined only by the balance between the initial jet inertia and the buoyancy:

$$L/D_j = \frac{1}{2} \cdot \frac{\rho_j}{\rho_c - \rho_j} \cdot Fr \ . \tag{6}$$

On the other hand, when the resistant force becomes much stronger than the buoyancy, Interaction Parameter K_i becomes infinite and then Panagration Parameter K_p becomes zero, and this means that the jet cannot penetrate into the coolant steadily.

The same discussions can be made for the case of the injection of the heavier jet into lighter coolant. In this case, however, if the resistant force due to the thermal and hydrodynamic interactions are smaller than the gravitational force due to the density difference between the jet and the coolant, the external forces acting on the jet stream cannot balance the initial jet inertia, and this means that the jet continues to penetrate into coolant down to the bottom of the pool under this condition. Therefore, to achieve the finite penetration depth steadily, the following condition is required:

$$\left(\frac{\Delta P}{\Delta l}\right)_f > (\rho_j - \rho_c)g \ , \tag{7}$$

that is,

$$K_i > 1 \ . \tag{8}$$

The interaction force $(\Delta P/\Delta l)_f$ is a kind of shear force acting on the jet surface, and, on the other hand, the gravitational force due to density and the jet inertia are the body forces. Therefore, it can be predicted that with increase of the jet diameter and density, it becomes impossible to balance these forces to achieve the finite penetration depth in the coolant. For example, the jet with large density and diameter (e.g. in the order of meter) postulated in whole core-melt down process in LWR severe accidents, may penetrate into coolant down to the bottom of the inlet plenum of the reactor vessel.

With increase of the resistant force due to the thermal and hydrodynamic interactions, Interaction Parameter K_i becomes larger and Penetration Parameter K_p approaches to zero, resulting in no penetration

of the jet into the coolant.

It is very difficult to determine the interaction force $(\Delta P/\Delta l)_f$ between the jet and the coolant during the penetration theoretically. From the experimental correlation for the penetration length of Eq. (1), the balance equation of Eq. (3) and Eq. (4), however, K_p & K_i can be obtained empirically as:

$$K_p = 4.2\ (\rho_c/\rho_j)^{0.5}(1-\rho_j/\rho_c)\ Fr^{-0.5}$$

$$= 4.2\ (\rho_c/\rho_j)^{0.5}(1-\rho_j/\rho_c)(Bo_j/We_j)^{0.5}\ , \qquad (9)$$

$$K_i = 1+\frac{1}{4.2}(\rho_j/\rho_c)^{0.5}(\rho_j/\rho_c-1)^{-1}(We_j/Bo_j)^{0.5}\ , \qquad (10)$$

where $Bo_j = \rho_j g D_j^2/\sigma_j$: Bond number,

and $We_j = \rho_j V_j^2 D_j/\sigma_j$: Weber number.

The Weber number, We_j is related to the breakup along the vertical trailing column of the jet caused by the Kelvin-Helmholtz type instability. Equation (10) indicates that with increase of We_j, the hydrodynamic interactions between the jet and the coolant become stronger, resulting in small penetration of the jet into the coolant.

On the other hand, the Bond number, Bo_j is related to the breakup at the leading edge of the jet which is caused by the Rayleigh-Taylor type instability. With increase of Bo_j, the interactions at the leading edge of the jet with the coolant become stronger, leading to a large amount of the vapor production, which makes the hydrodynamic interactions between the vertical trailing jet column with the coolant weaker by the thicker vapor blanket. Therefore, Interaction Parameter K_i becomes smaller with increase of Bo_j. When Bo_j is small, the lack of the vapor production at the jet leading edge causes the strong hydrodynamic interactions between the vertical trailing jet column and the coolant because of the thinner vapor blanket. And hence it becomes difficult for the jet to penetrate deeply into the coolant.

Equation (10) also indicates that with increase of the jet diameter and density, Interaction Parameter K_i approaches to 1. This means that it becomes impossible to achieve the finite penetration depth as predicted in the previous section.

The experimental results of K_p and K_i are shown in Fig. 11 and 12,

respectively. From this figure, it is seen that most of the penetration lengths in the cases of the hot water jet injected into freon-11 are lower by one order than those predicted only by the balance between the initial jet inertia and the buoyancy.

Interaction parameters of experiments by Spencer et al.[10] are also plotted in Fig. 12, which are much smaller than those of the present experiments. This means that the thermal and hydrodynamic interactions between the jet and the coolant are stronger in the water jet injected into liquid nitrogen and freon-11 than in the heavy metal jet injected into water.

IV. SUMMARY AND CONCLUSIONS

A series of the model experiments is in progress at PNC at low (<500 °C) and high (1000 ∿ 2300 °C) temperatures to investigate the key phenomenology during the relocation processes of the molten core materials, such as thermal and hydrodynamic interactions between the molten core jets released from the bottom of the core assembly and the coolant/structures.

As the first series of the experiments to study the fundamental physical phenomena of the penetration behaviors of a large molten jet into coolant, the experiments at low temperature have been performed by using a (hot) water jet, freon-11 and liquid nitrogen pools. A hot water jet was injected into freon-11 at room temperature with various jet velocities from 2.5 m/sec to 15 m/sec through a nozzle with various diameters from 5 mm to 40 mm. To examine the effects of the density difference between the jet and the coolant on the jet penetration behaviors, additional experiments were performed with a water jet at room temperature and the liquid nitrogen pool. The penetration behaviors of the jet into coolant were observed by a high-speed video camera with 200 frames per second.

The experimental results are summarized as follows:

(1) It is clearly seen that the instability produced by the vapor flow which is generated by the thermal interaction between the hot jet and coolant tends to break up the jet and that in turn the blanketing the jet by the vapor helps the penetration of the jet into the coolant.

(2) The penetration length of the jet into coolant tends to increase

with the jet velocity, the jet diameter and the density ratio between the jet and coolant. It, however, becomes much shorter because of the thermal and hydrodynamic interactions between the jet and the coolant. The relative penetration length normalized by the jet diameter can be correlated well with the Froude number and the density ratio between the jet and the coolant:

$$L/D_j = 2.1\ (\rho_j/\rho_c)^{0.5}\ Fr^{0.5}\ .$$

This correlation can also predict well the experimental results of the breakup length which were obtained by Spencer et al. with hot and very heavy jets such as Wood's metal injected into the water pool.

From the present experiments, it is concluded that the behaviors of the vapor generated by the thermal interactions between the jet and the coolant play an important role in the penetration process of the hot jet into coolant. In the case of the mild FCIs such as present experiments, the jet blanketing by the vapor generated at the leading edge of the jet due to the Rayleigh-Taylor type instability tends to prevent the jet from contacting with the coolant at the vertical trailing column of the jet, which helps the jet to penetrate into the coolant. On the other hand, the Kelvin-Helmholtz type instability increases the hydrodynamic interactions between the vertical trailing jet column and the coolant, which results in small penetration of the jet into the coolant.

From the viewpoint of jet and coolant mixing behaviors, the density difference of two fluids is of primary importance. Both densities are much closer in the present experiments than in the prototypical case, and hence the present experiments correspond to higher mixing and lower penetration cases. On the other hand, in reactor cases the heat transfer between the jet and the coolant will be higher and the radiation would make the jet penetration behaviors quite different from the present experiments with weak radiation effects.

Therefore, to extrapolate the present results to the reactor accident conditions, additional experimental data are required and being prepared at PNC under conditions of larger density difference between the jet and coolant, larger jet diameter, higher temperature of the jet and energetic FCI.

ACKNOWLEDGMENTS

The authors would like to express their appreciations to Messrs. N. Ushiki, S. Sato and the other members of SAG-3 Group of FBR Safety Engineering Section, PNC for their technical contributions to the present study.

The support of the section manager, Mr. N. Tanaka is gratefully acknowledged.

NOMENCLATURE

Bo_j	:	Bond number ($= \rho_j g D_j^2/\sigma_j$)
D_j	:	Initial jet density
Fr	:	Froude number ($= V_j^2/gD_j$)
g	:	Gravitational acceleration
K_i	:	Interaction Parameter defined by Eq. (5)
K_p	:	Penetration Parameter defined by Eq. (4)
L	:	Mean penetration length
$(\frac{\Delta P}{\Delta l})_f$	:	Resistant force due to thermal and hydrodynamic interactions between jet and coolant
V_j	:	Initial jet velocity
We_j	:	Weber number ($= \rho_j V_j^2 D_j/\sigma_j$)
ρ_c	:	Density of coolant
ρ_j	:	Density of jet
σ_j	:	Surface tension of jet

REFERENCES

1. J.S.W. Rayleigh, Proc. Lond. Math. Soc. 10 (1978)4
2. K. Weber, Z. angew. Math. Mech., 11 (1931) 136
3. R.W. Fenn III and S. Middleman, "Newtonian Jet Stability: The Role of Air Resistance," AIChE Journal, 15 (1969) 379
4. R.P. Grant and S. Middleman, "Newtonian Jet Stability," AIChE Journal, 12 (1966) 669
5. R.E. Phinney, "Stability of a Laminar Viscous Jet - The Influence of the Initial Disturbance Level," AIChE Journal, 18 (1972) 432

6. B.J. Meister and G.F. Sheele, "Prediction of Jet Length in Immiscible Liquid Systems," AIChE Journal, 15 (1969) 689
7. M.J. McCarthy and N.A. Molloy, "Review of Stability of Liquid Jets and the Influence of Nozzle Design," The Chemical Eng. Journal, 7 (1974) 1-20
8. T.G. Theofanous and M. Saito, "An Assessment of Class-9 (Core-Melt) Accident for PWR Dry-Containment Systems," Nuclear Engineering and Design, 66 (1981) 301-332
9. K. Marten, V. Casal and K.J. Mack, "Model Experiments to Study the Stability of a Fuel Jet in Sodium," Proc. Int. Conf. Science and Technology of Fast Reactor Safety, Vol.2, (1986) 607
10. B.W. Spencer, J.D. Gabor and J.C. Cassulo, "Effect of Boiling Regime on Melt Stream Breakup in Water," 4th Miami Int. Symp. on Multi-phase Transport & Particulate Phenomena, (1986)
11. R.H. Bradley and L.C. Witte, "Explosive Interaction of Molten Metals Injected into Water," Nuclear Science and Engineering, 48 (1972) 387
12. M. Epstein and H.K. Fauske, "Steam Film Instability and the Mixing of Core-melt Jets and Water," ANS Proc. 1985 Nat'l Heat Transfer Conf. ANS #700101, (1985)
13. T.G. Theofanous, B. Najafi and E. Rumble, "An Assessment of Steam-Explosion-Induced Containment Failure. Part I: Probabilistic Aspects," Nuclear Science and Engineering, 97, (1987) 259-281

Table 1 Experimental conditions (I)

Water jet into freon-11*

Experimental No.	Experimental Conditions			
	Jet			Coolant
	Diameter (mm)	Initial Velocity (m/s)	Temperature (°C)	Temperature (°C)
II-W•R11-B5-01	5	2.5	90.0	8.0
-08	5	2.9	90.5	18.9
-03	5	5.2	90.0	3.0
-09	5	5.2	92.7	17.6
-04	5	9.0	90.0	4.0
-05	5	9.0	90.0	4.0
-06	5	9.0	90.0	2.0
-11	5	9.0	90.3	18.9
-14	5	9.0	90.0	21.7
-07	5	14.9	90.0	17.9
-12	5	14.9	89.7	21.6
-13	5	14.9	91.2	17.0
-15	5	14.9	90.9	19.4
-16	5	14.9	90.7	19.1
-B4-01	10	3.5	90.0	6.0
-05	10	3.9	90.4	13.4
-02	10	5.1	90.0	5.0
-03	10	5.1	90.0	23.2
-06	10	10.2	91.9	14.4
-B3-01	20	4.3	90.0	14.0
-05	20	4.7	90.6	22.0
-02	20	5.1	90.0	14.0
-04	20	5.1	90.0	5.0
-07	20	10.6	89.7	14.4
-B2-02	30	5.5	90.8	22.0
-03	30	5.5	90.0	21.2
-06	30	6.8	90.0	20.5
-05	30	9.4	90.1	22.4
-B1-02	40	5.5	89.8	6.5
-03	40	5.5	90.2	17.0
-04	40	6.7	90.2	12.1

* Boiling point at 1 atm : 23.8°C

Table 2 Experimental conditions (II)

Water jet into liquid nitrogen

Experimental No.	Experimental Conditions			
	Jet			Coolant
	Diameter (mm)	Velocity (m/s)	Temperature (°C)	Temperature (°C)
II-W•LN_2-B5'-02	4.4	2.5	∿10	-195.8
-B5 -08	5	2.9	14.5	-195.8
-05	5	5.2	19.1	-195.8
-06	5	9.0	18.4	-195.8
-09	5	9.0	15.0	-195.8
-B4'-02	11.1	3.5	∿10	-195.8

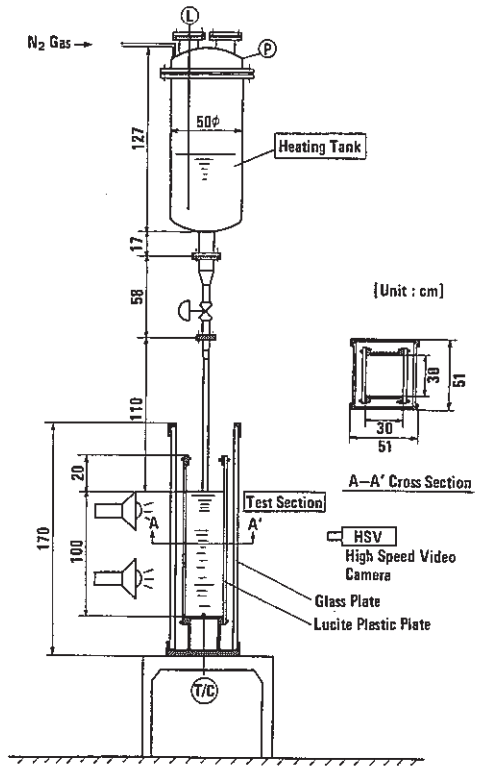

Fig. 1 JET-I Experimental Facility

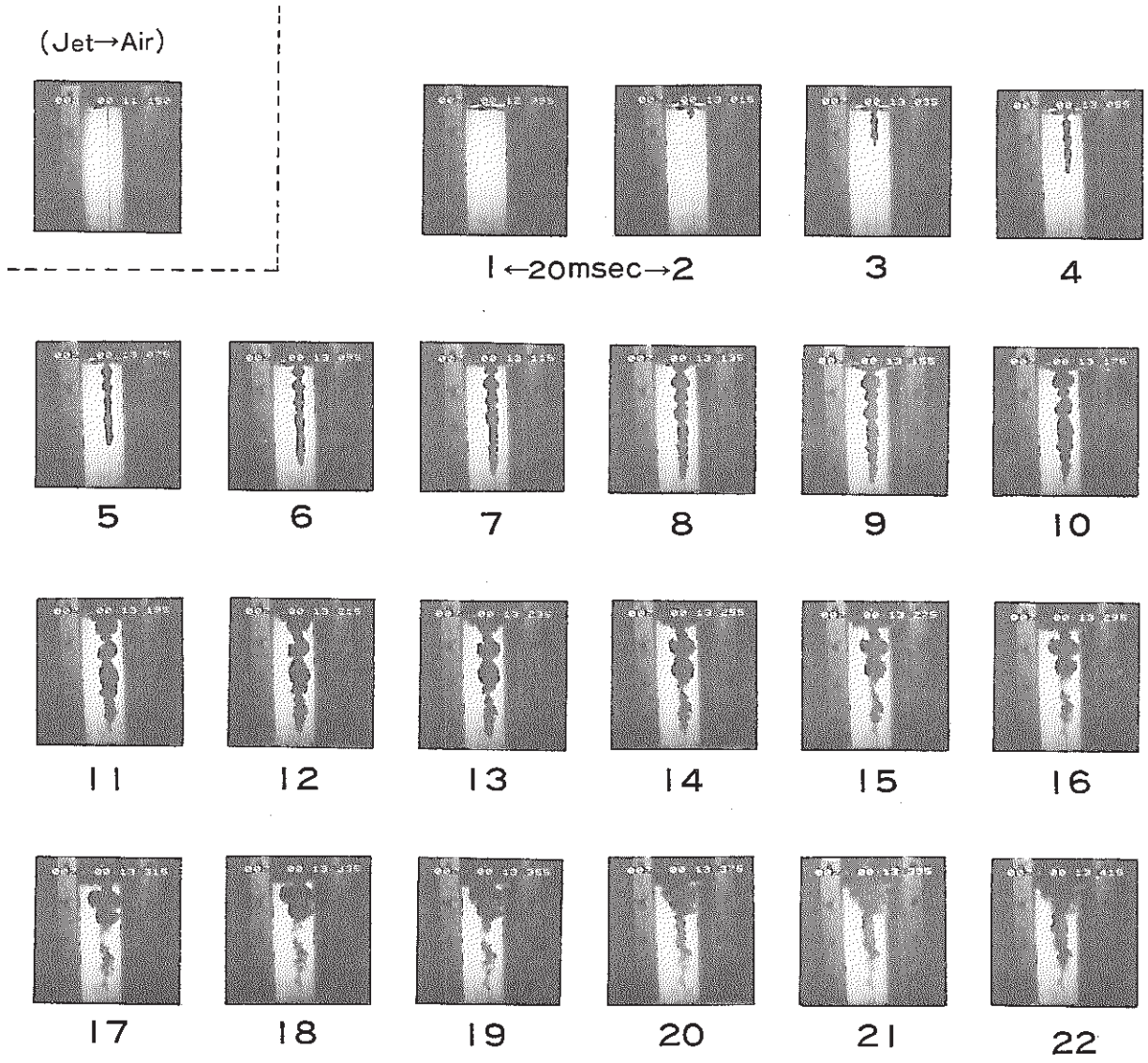

Fig. 2 Initial Penetration Behaviors of Hot Water Jet into Freon-11 (Jet: Temp. 90°C, Diameter 5mmφ, Velocity 9m/sec)

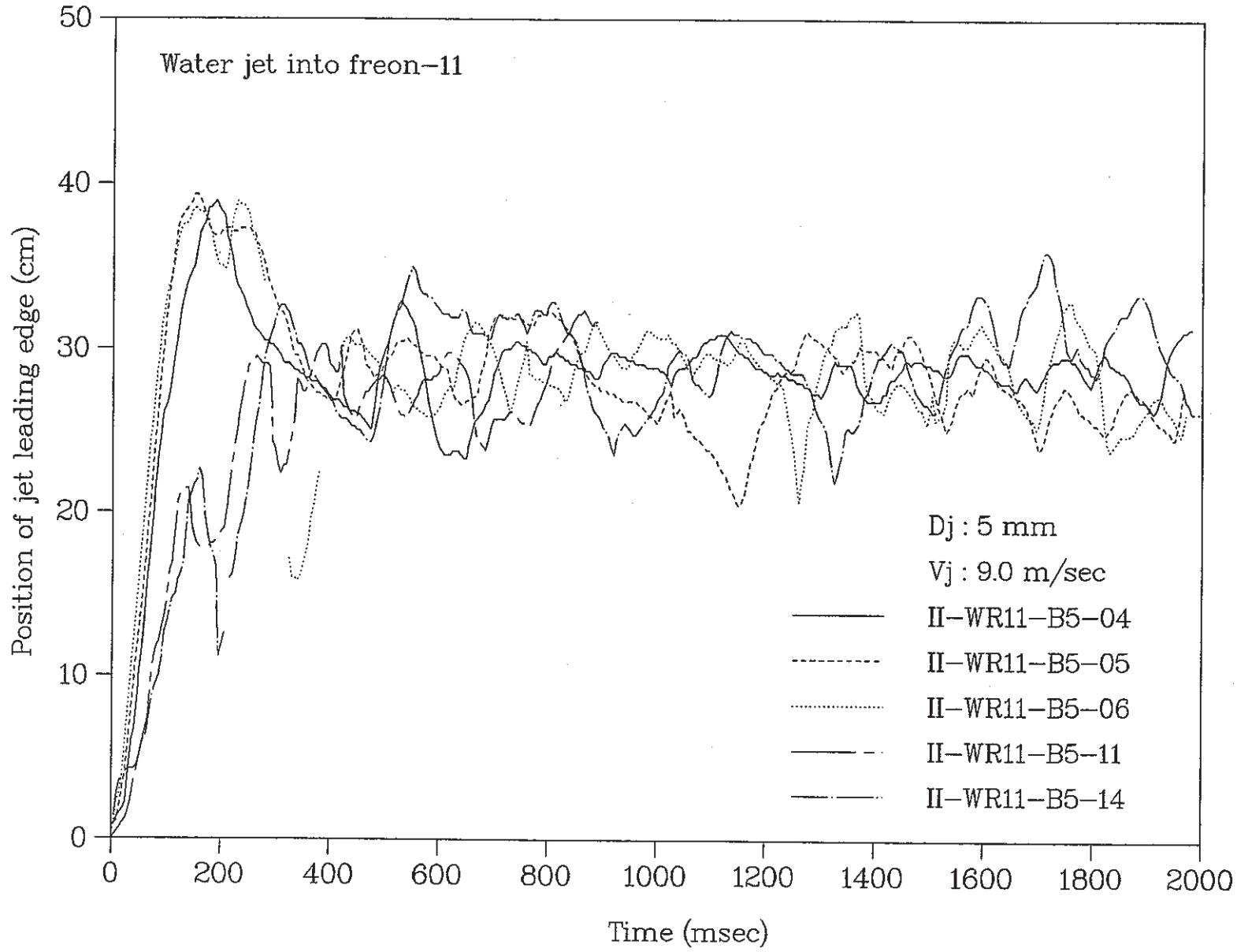

Fig. 3 Reproducibility of jet penetration behaviors

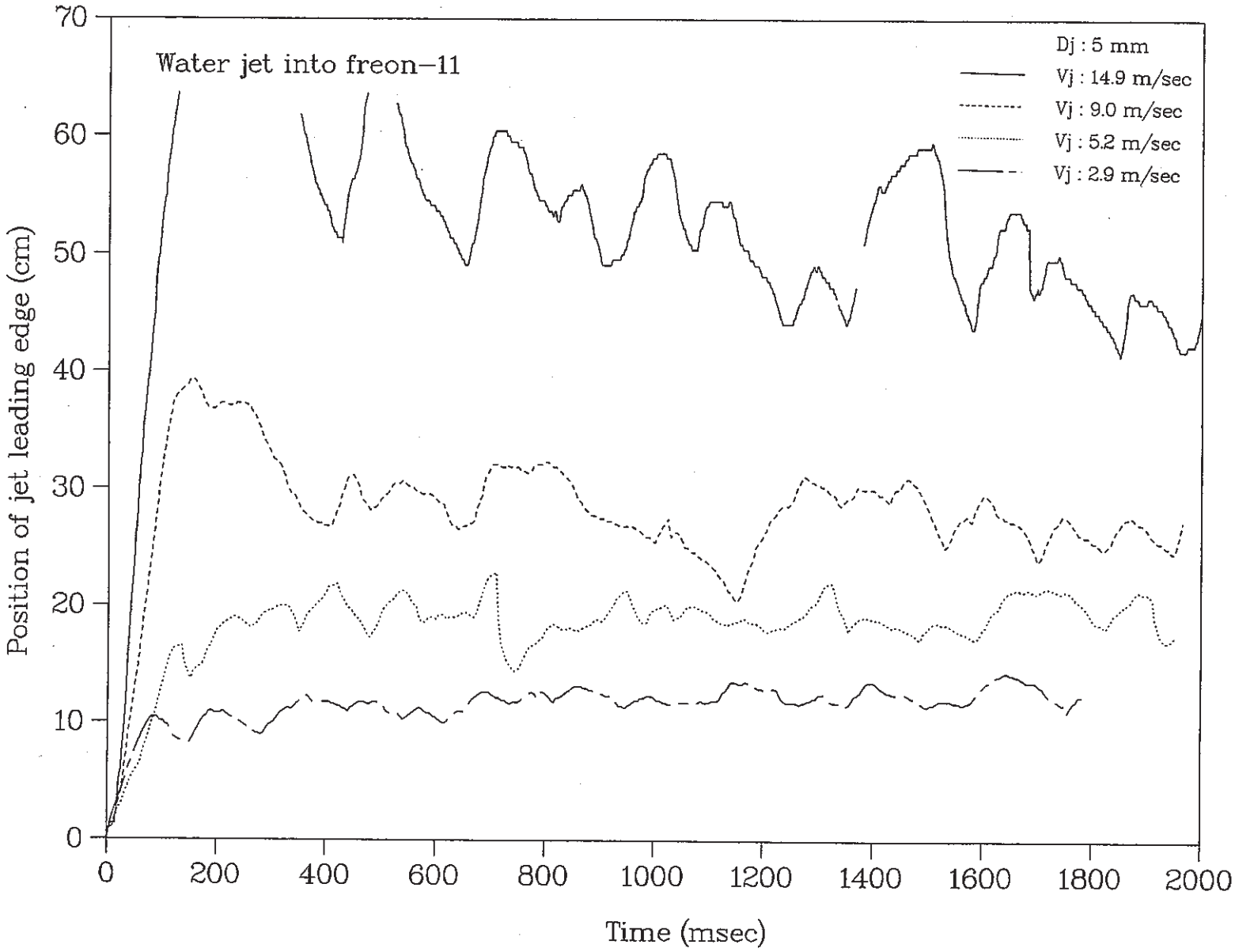

Fig. 4 Effects of jet velocity on penetration behaviors (in freon-11)

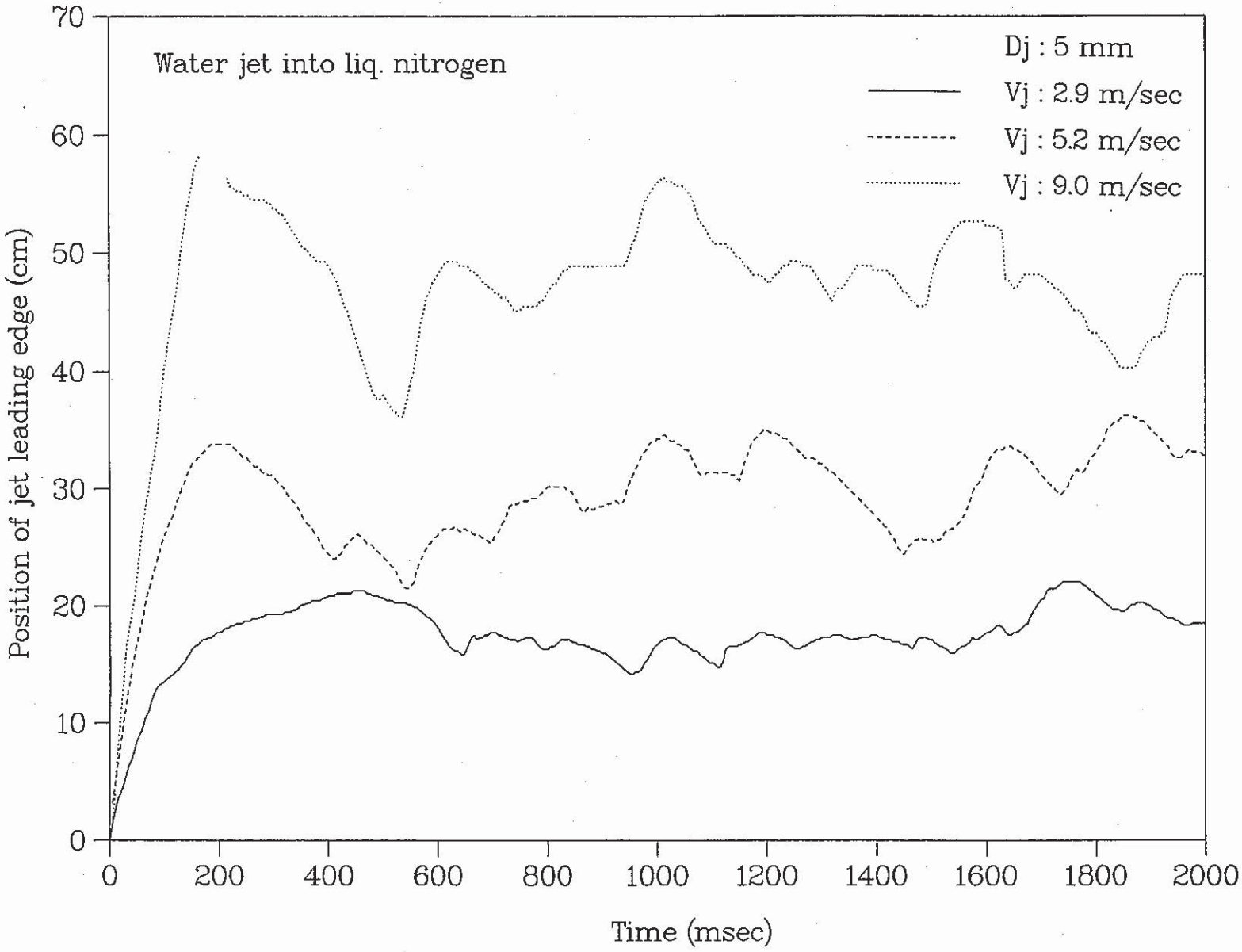

Fig. 5 Effects of jet velocity on penetration behaviors (in liquid nitrogen)

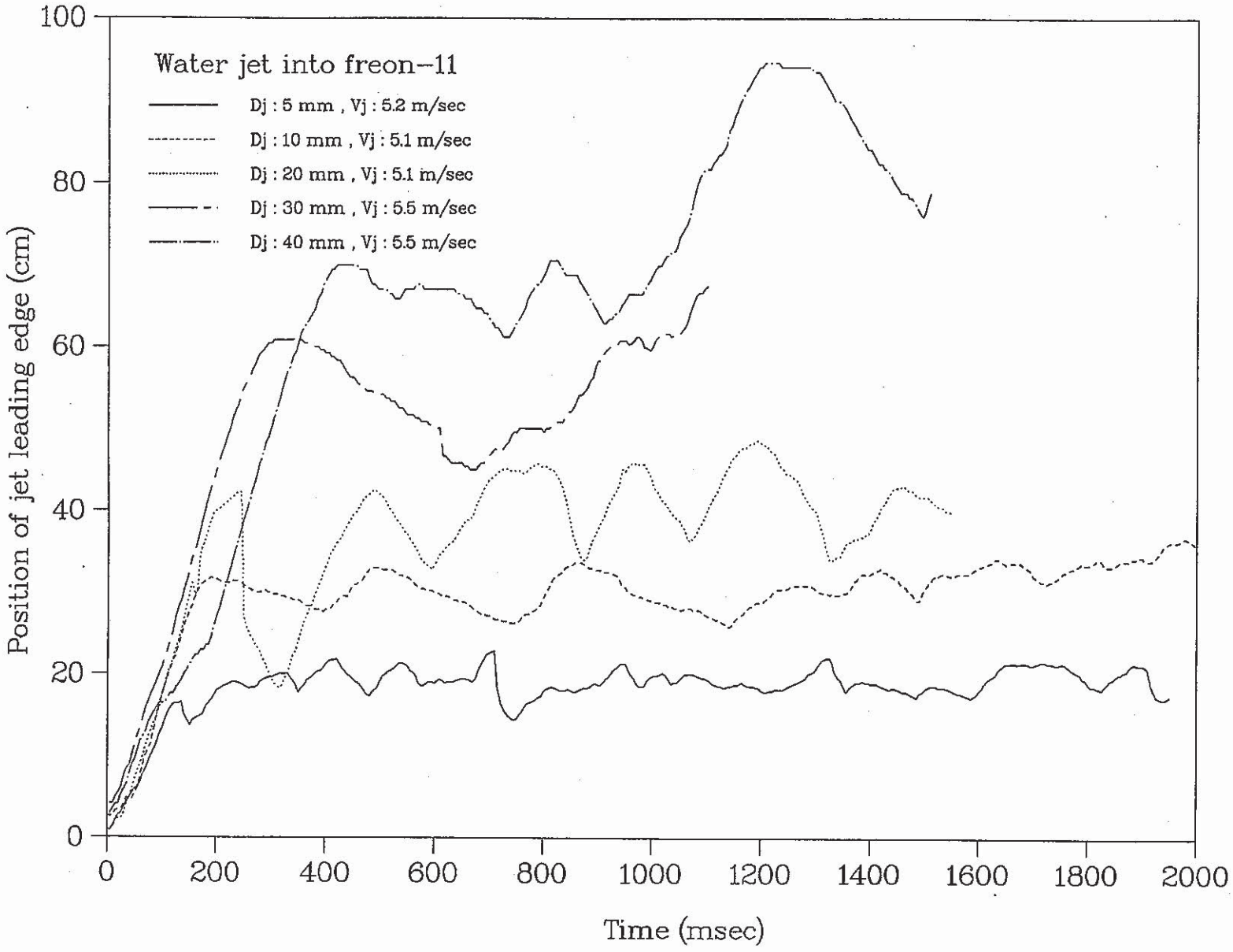

Fig. 6 Effects of jet diameter on penetration behaviors (in freon-11)

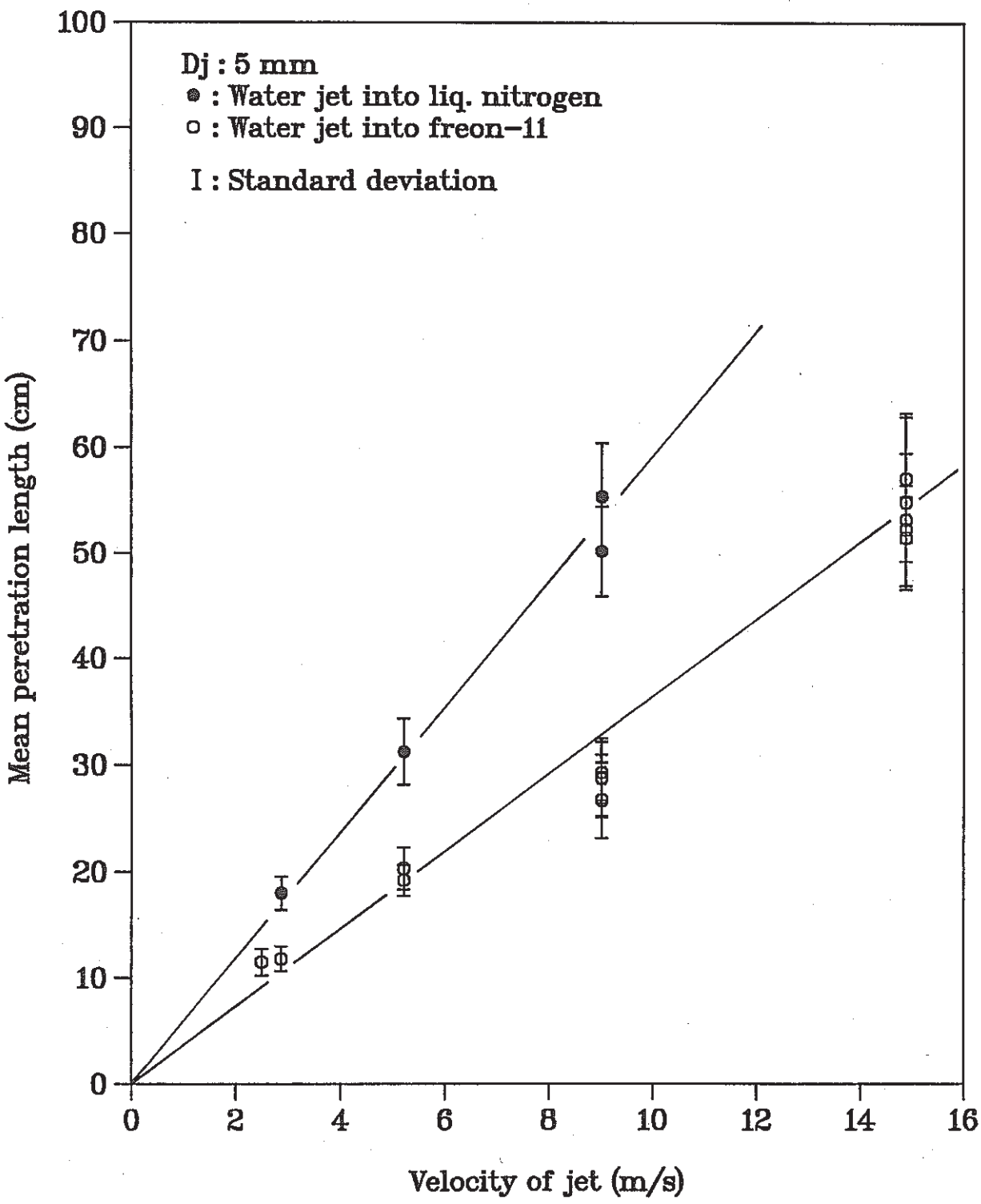

(a) Jet diameter: 5 mm

Fig. 7 Influences of jet velocity, jet diameter and density ratio of jet to coolant on jet mean penetration lengths

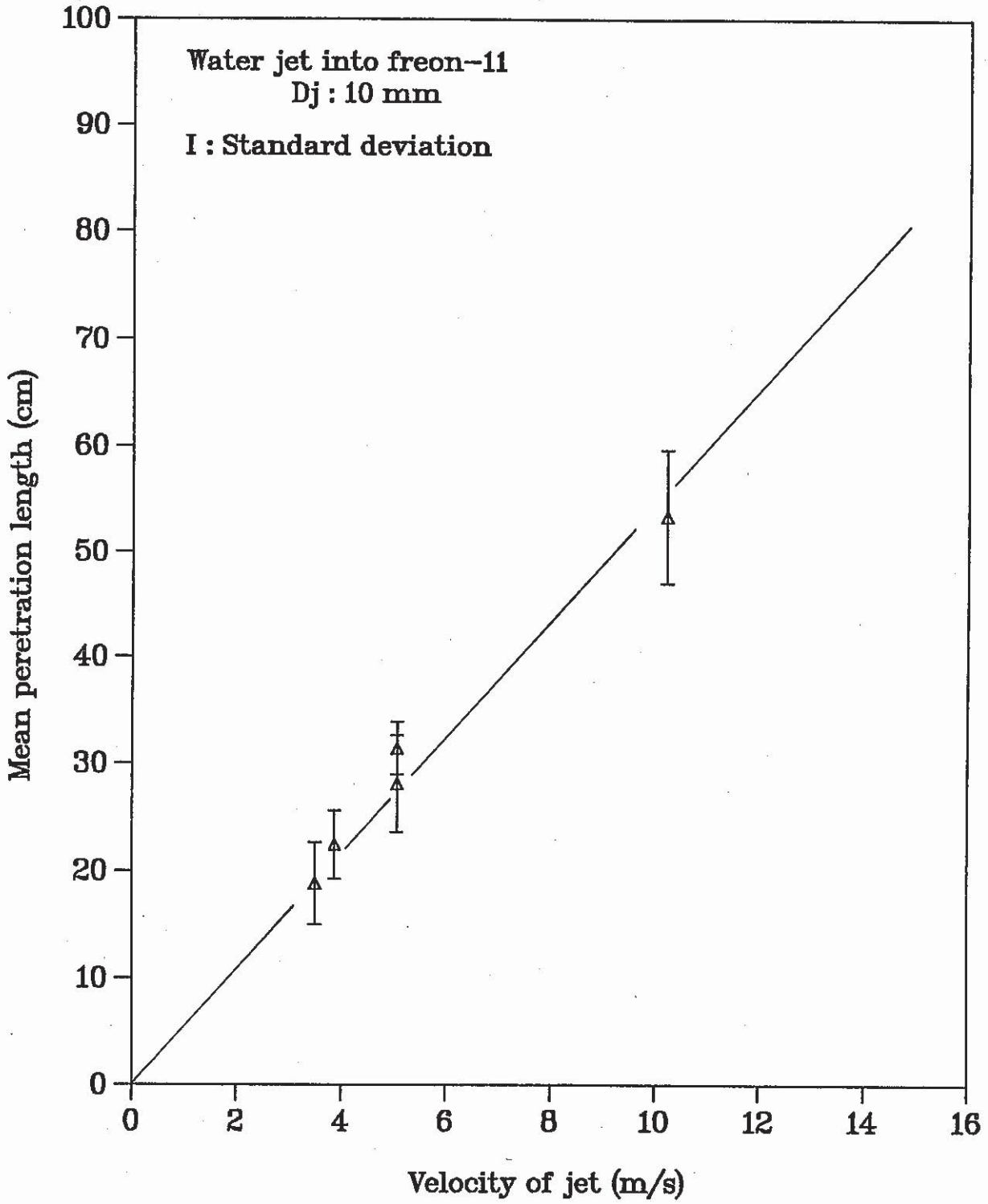

(b) Jet diameter: 10 mm

Fig. 7 (contd.)

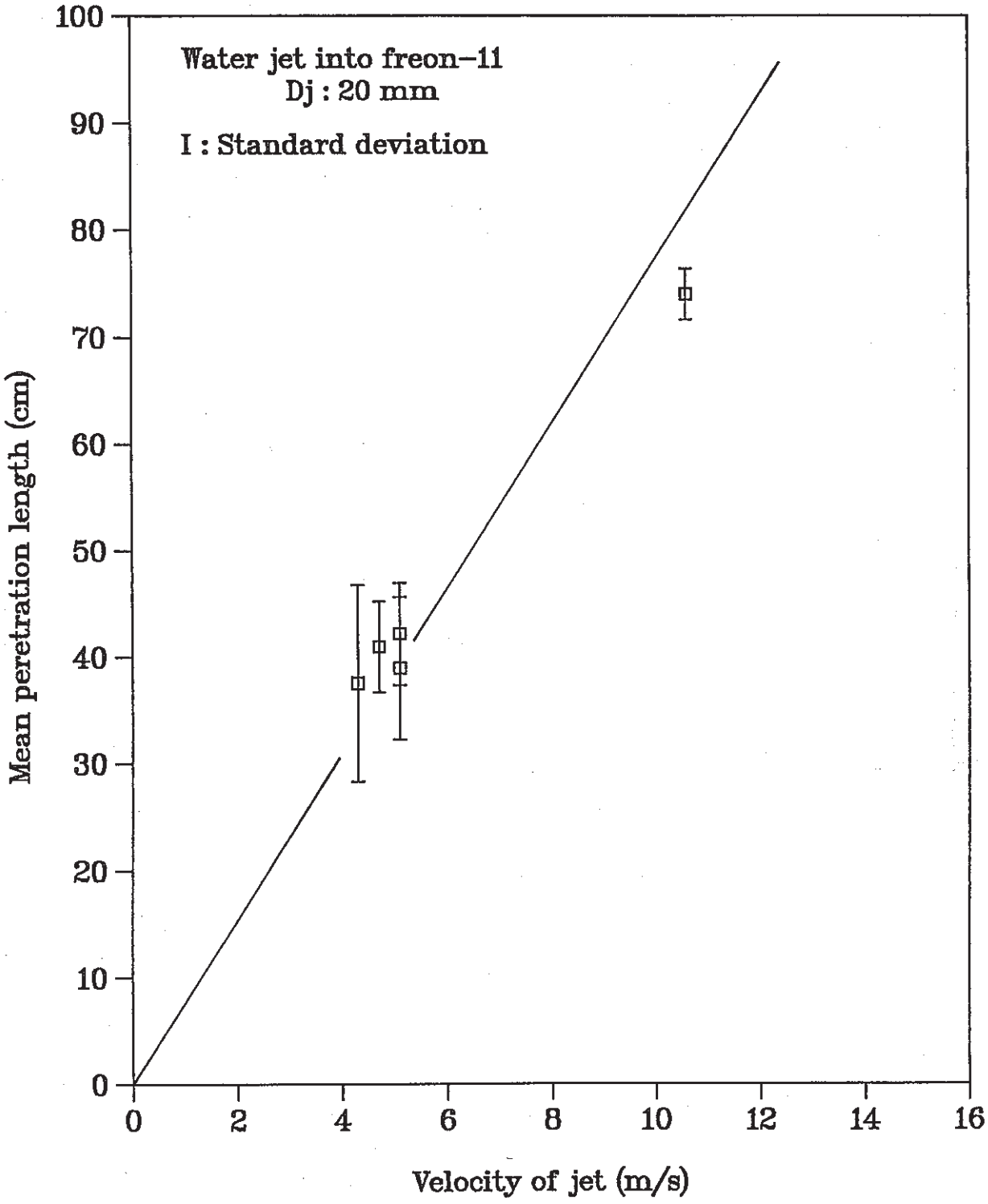

(c) Jet diameter: 20 mm

Fig. 7 (contd.)

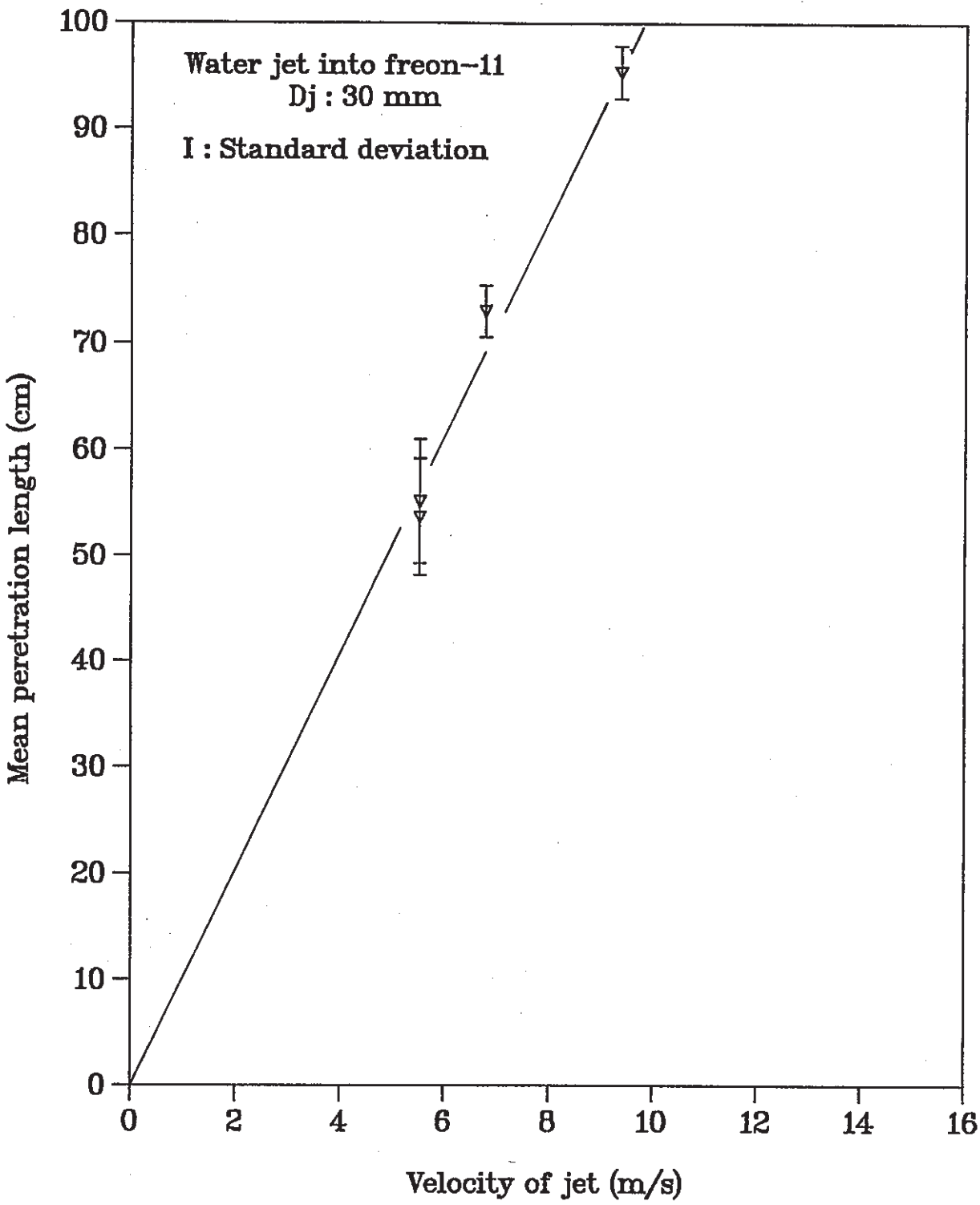

(d) Jet diameter: 30 mm

Fig. 7 (contd.)

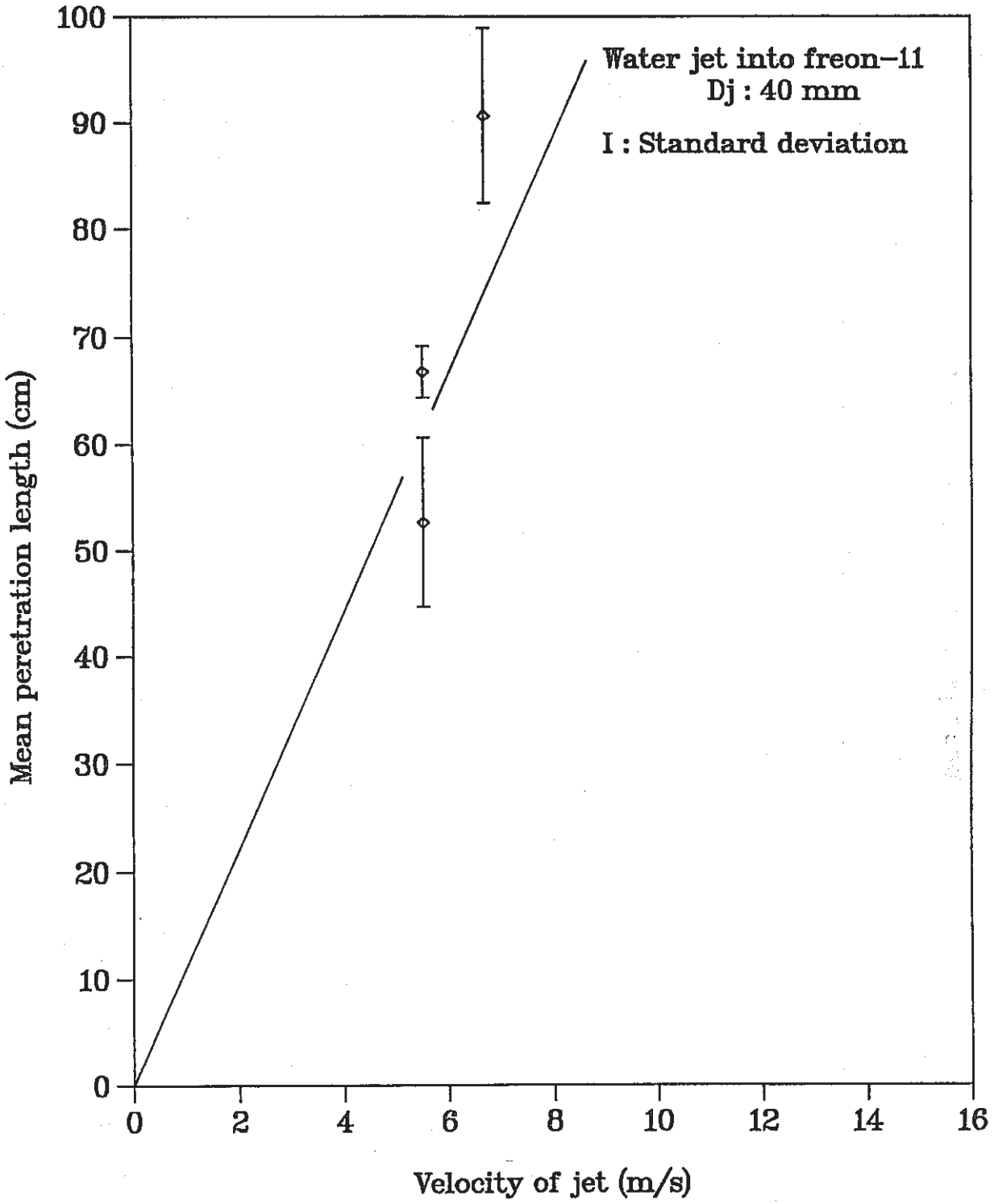

(e) Jet diameter: 40 mm

Fig. 7 (contd.)

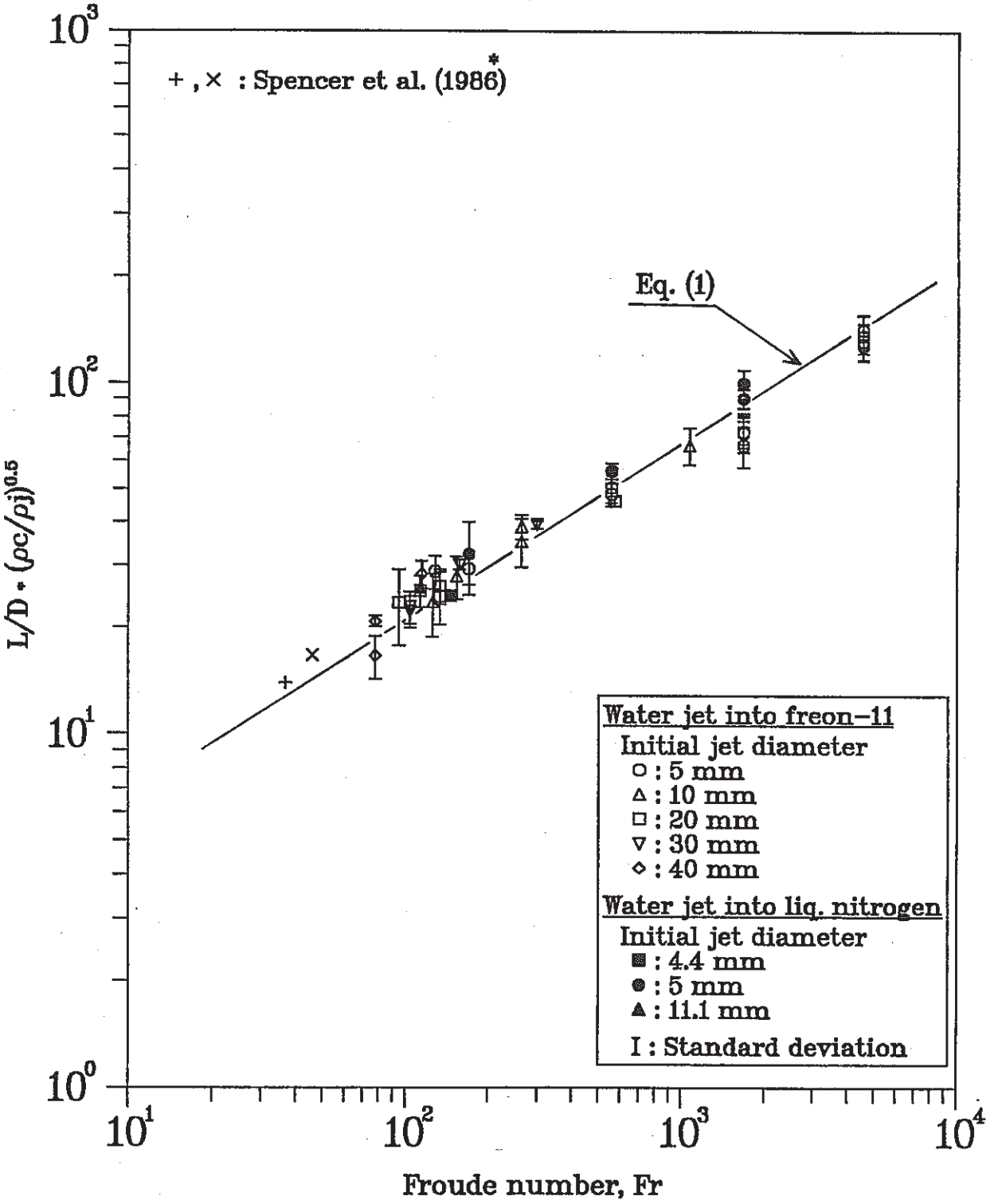

Fig. 8 Experimental correlation on jet mean penetration length

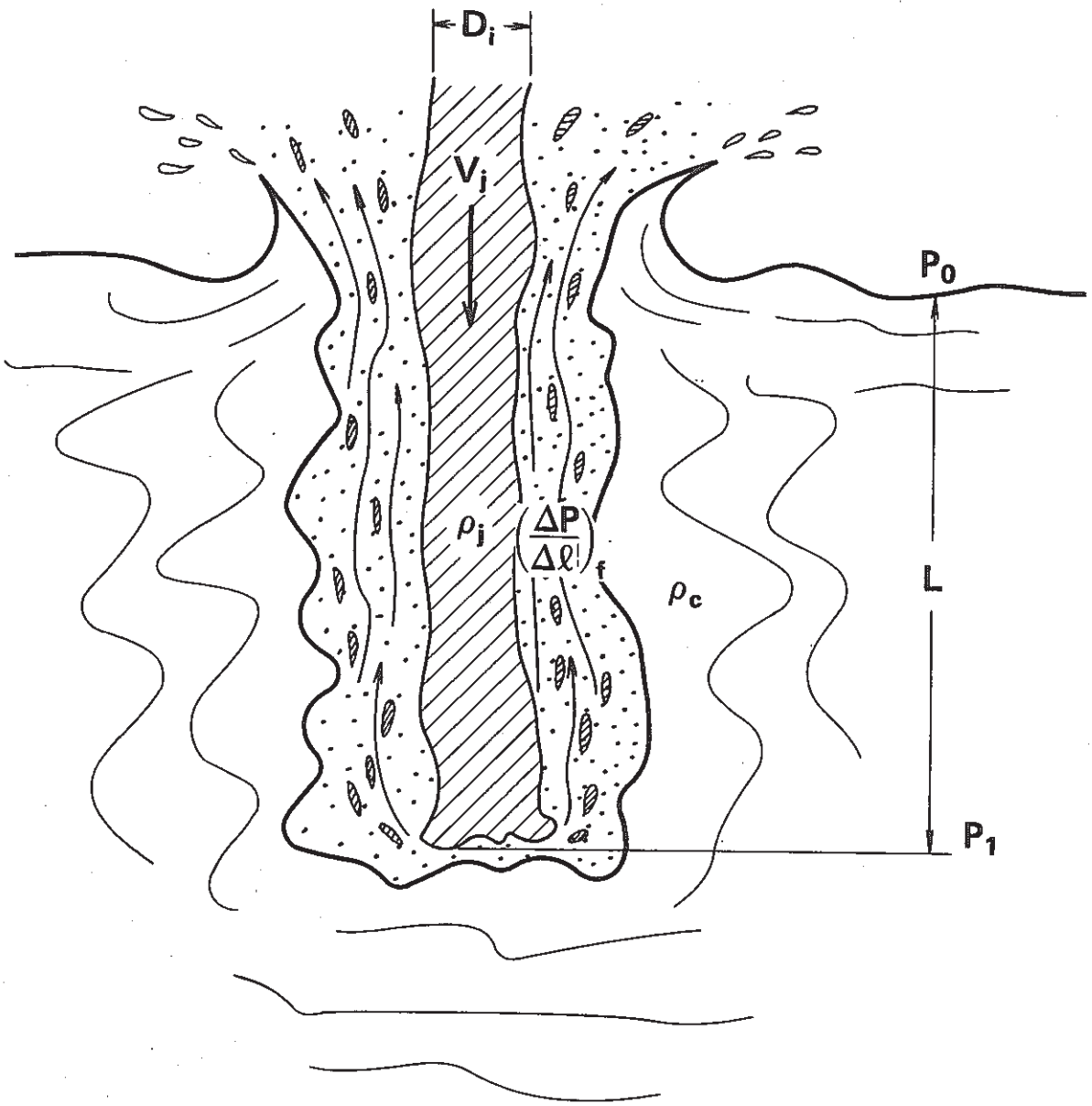

$$\frac{1}{2}\rho_j V_j^2 = (\rho_c - \rho_j)gL + \left(\frac{\Delta P}{\Delta \ell}\right)_f L$$

$$\therefore\ L/D_j = \frac{1}{2}\cdot\left(\frac{\rho_j}{\rho_c - \rho_j}\right)\cdot F_r \cdot K_p$$

where

$F_r \equiv V_j^2/gD_j$: Froude Number

$K_p \equiv 1/(1-K_i)$: Penetration parameter

$K_i \equiv \left(\frac{\Delta P}{\Delta \ell}\right)_f / (\rho_j - \rho_c)g$: Interaction parameter

Fig. 9 Schematic of jet penetration behaviors into coolant

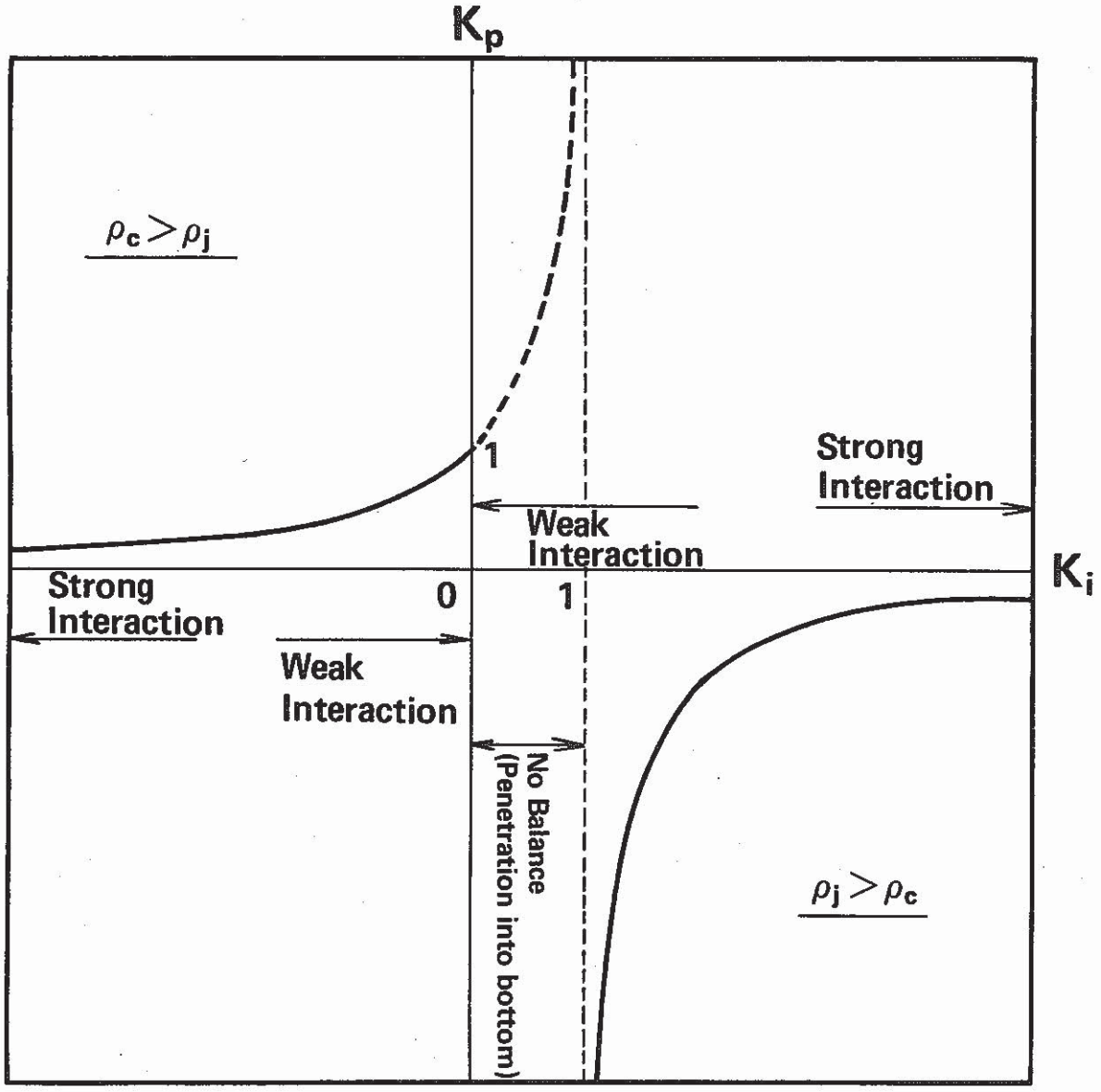

Fig. 10 Relationship between Penetration Parameter (K_p) and Interaction Parameter (K_i)

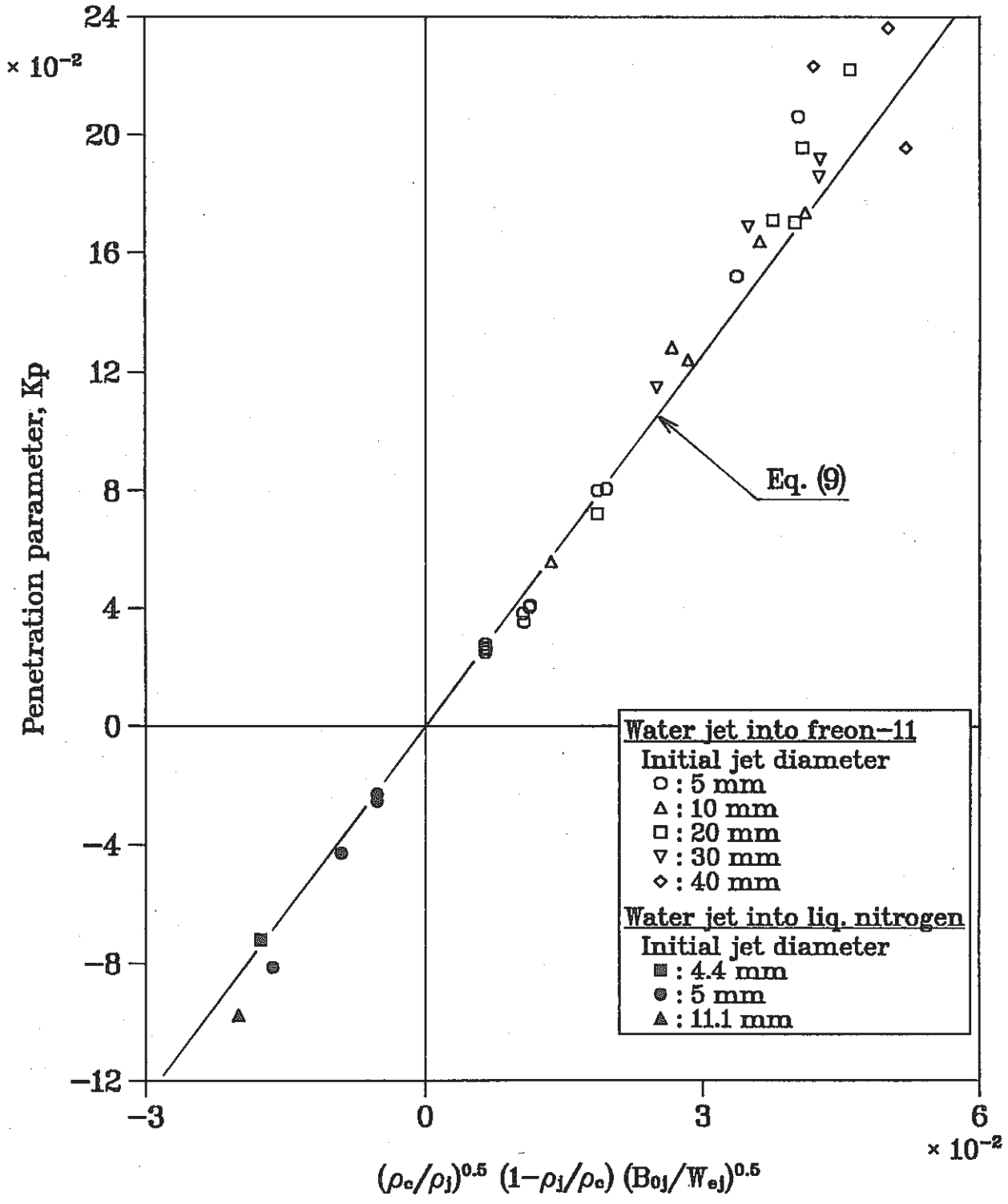

Fig. 11 Experimental correlation of Penetration Parameter, K_p

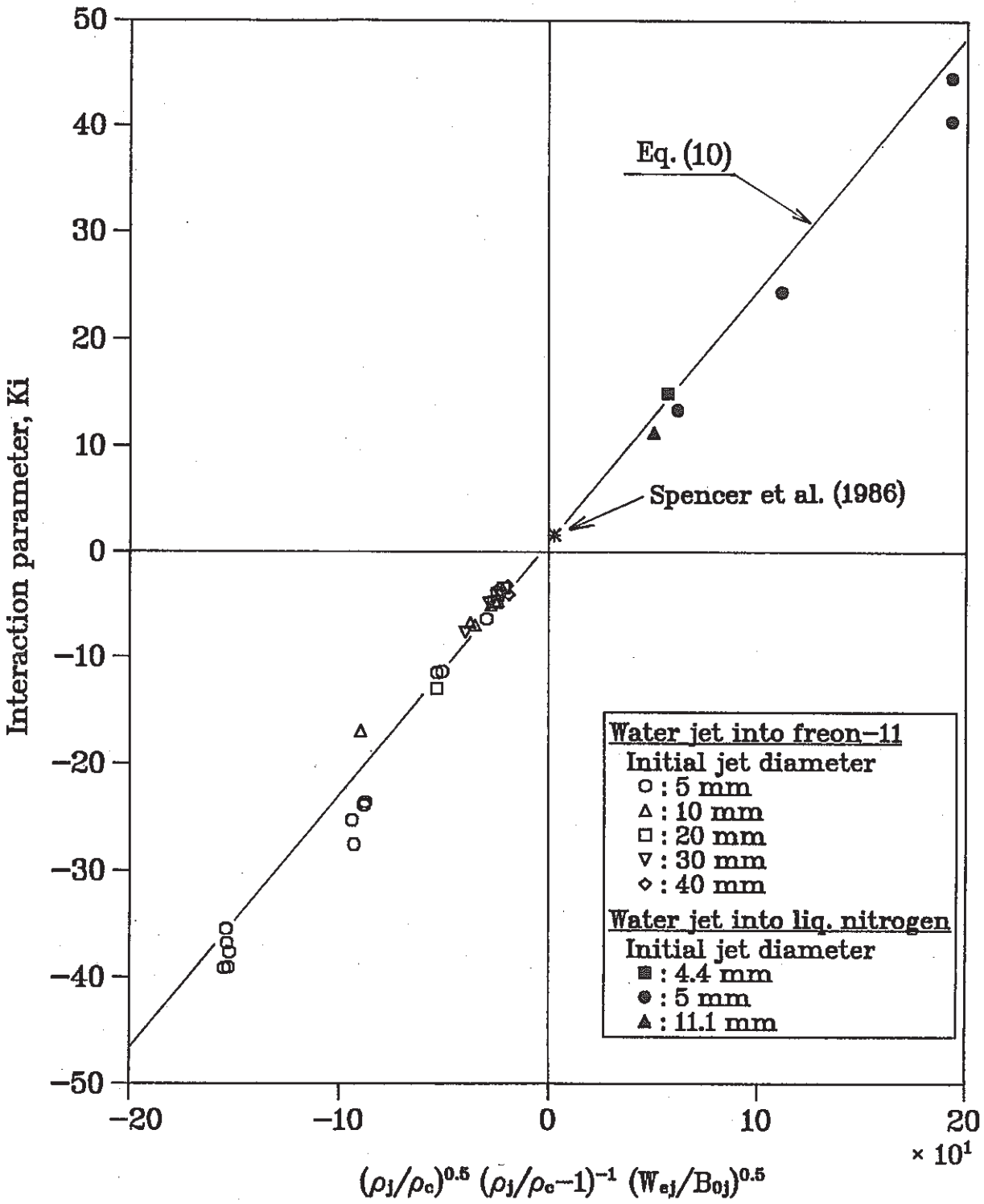

Fig. 12 Experimental correlation of Interaction Parameter, K_i